



Universiteit
Leiden
The Netherlands

The road to Insurmountability: Novel avenues to better target CC Chemokine Receptors

Ortiz Zacarías, N.V.

Citation

Ortiz Zacarías, N. V. (2019, December 4). *The road to Insurmountability: Novel avenues to better target CC Chemokine Receptors*. Retrieved from <https://hdl.handle.net/1887/81379>

Version: Publisher's Version

License: [Licence agreement concerning inclusion of doctoral thesis in the Institutional Repository of the University of Leiden](#)

Downloaded from: <https://hdl.handle.net/1887/81379>

Note: To cite this publication please use the final published version (if applicable).

Cover Page



Universiteit Leiden



The handle <http://hdl.handle.net/1887/81379> holds various files of this Leiden University dissertation.

Author: Ortiz Zacarías, N.V.

Title: The road to Insurmountability: Novel avenues to better target CC Chemokine Receptors

Issue Date: 2019-12-04

Chapter 6

Design and characterization of an intracellular covalent ligand for CC Chemokine Receptor 2 (CCR2)



Natalia V. Ortiz Zacarías, Julien Louvel, Tereza Šimková, Kirti K. Chahal, Yi Zheng, Emy Theunissen, Lloyd Mallee, Daan van der Es, Tracy Handel, Irina Kufareva, Adriaan P. IJzerman, Laura H. Heitman

Manuscript in preparation



ABSTRACT

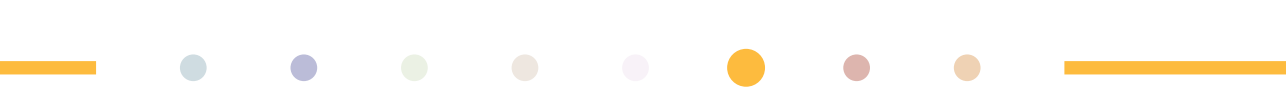
CC chemokine receptor 2 (CCR2) plays a key role in the migration of leukocytes to sites of inflammation; thus, CCR2 represents a potential drug target in many inflammatory and immune diseases. Yet all CCR2 antagonists developed so far have failed in clinical trials (mostly) due to lack of efficacy, rendering the development of novel tools and concepts necessary to better study drug receptor pharmacology in early phases of drug discovery. In this regard, the recent crystal structure of CCR2 has suggested a new manner of pharmaceutical intervention, i.e. using intracellular allosteric modulators. In addition, irreversible or covalent probes represent important pharmacological tools that allow a variety of applications: target crystallization, study of *in vivo* target engagement or target validation, among others. Thus, we aimed to develop and characterize an intracellular covalent ligand for CCR2. Based on the structure of a known CCR2 intracellular ligand, SD-24, we designed and synthesized several potential covalent ligands by incorporating different electrophilic groups as reactive warheads. Next, a combination of radioligand binding and functional assays allowed us to identify compound **14** as an intracellular covalent binder for CCR2. In addition, *in silico* modeling followed by site-directed mutagenesis of CCR2 confirmed that **14** binds to the intracellular pocket of CCR2, where a cysteine residue appears to be one of the target amino acids for the irreversible interaction. To conclude, we report the design, synthesis, pharmacological characterization and binding mode of **14**, a first covalent probe for CCR2. This tool compound might represent a promising approach to further study CCR2, both *in vitro* and *in vivo*.

INTRODUCTION

CC Chemokine receptor 2 (CCR2) is a G protein-coupled receptor (GPCR) expressed on the surface of various immune cells, including monocytes, basophiles and natural killer cells.¹ Activation of CCR2 by its endogenous chemokine ligands, such as CCL2, CCL7 and CCL13, results in leukocyte trafficking towards sites of inflammation as part of the immune response.² However, dysregulation of CCR2 signalling can lead to leukocyte accumulation—a hallmark of the inflammatory response—and ultimately to a variety of inflammatory and immune diseases.³ In this regard, preclinical studies have suggested a critical role of CCR2/CCL2 signalling in atherosclerosis (**Chapter 7**),⁴ diabetes,⁵ neuropathic pain,⁶ and cancer,⁷ among others. Although many efforts have been made to bring CCR2 antagonists into the clinic, most clinical candidates have failed due to lack of efficacy.⁸ Thus, a better understanding of its structure and biological function, both *in vitro* and *in vivo*, is necessary for the successful development of CCR2 antagonists.

Covalent ligands have recently re-emerged as valuable tool compounds, i.e. covalent probes or affinity-based probes, and as therapeutic agents for several targets and diseases.⁹⁻¹¹ As the name implies, covalent ligands contain a reactive group, or “warhead”, which allows them to bind to their target in an irreversible manner.¹² In the field of GPCRs, covalent ligands have been mostly used as tool compounds due to major safety concerns; however, recent studies have highlighted several potential advantages for the development of covalent drugs, including their insurmountability and prolonged duration of action.¹³⁻¹⁵ As tool compounds, covalent ligands have been increasingly used for structure elucidation purposes, as they stabilize the inherently flexible receptor-ligand complexes.⁹ Examples include the recent crystal structures of cannabinoid receptor CB₁,¹⁶ and adenosine A₁ receptor.¹⁷ Furthermore, covalent probes represent valuable starting points for a wide variety of chemical biology and proteomic profiling applications.^{9, 12}

Recently, the X-ray structures of CCR2 isoform a (CCR2a)¹⁸ and isoform b (CCR2b, **Chapter 3**)¹⁹ have been solved in complex with small-molecule antagonists. Besides providing structural insight on the antagonists' binding mode, the crystal structure of CCR2b described in **Chapter 3** has revealed an intracellular binding site for small molecules, which can be used to inhibit CCR2 without directly competing with the binding of chemokines.¹⁹ Due to their noncompetitive manner of inhibition, these intracellular allosteric modulators might be more efficacious in the treatment of inflammatory diseases characterized by high levels of endogenous chemokines, as suggested in **Chapter 2**.²⁰ An intracellular covalent ligand could represent a valuable tool to further investigate CCR2 pharmacology and intracellular modulation. Thus, based on previously described high-affinity intracellular ligands for CCR2, we aimed to design and synthesize novel putatively covalent intracellular ligands for this



receptor. Biochemical characterization, *in silico* modelling and a mutational study resulted in the identification of compound **14** as a covalent, negative allosteric modulator (NAM) of CCR2, and as a promising starting point for a variety of applications to further study CCR2 pharmacology.

RESULTS

Design and apparent affinity of putative covalent ligands for CCR2

As a starting point for the design of putative covalent intracellular ligands for CCR2, we first synthesized sulfonamide **34** by Peace *et al.*,²¹ corresponding to compound **7** in our study (Figure 1). In order to covalently target nucleophilic residues present near the intracellular binding pocket of CCR2, four different warheads with different reactivity profiles were envisioned: fluorosulfonyl, acryloyl, isothiocyanate, and thiocyanate. These reactive warheads were incorporated at the position of the carboxyl group of **7**, using an ethylacetamide linker (Figure 1). Lastly, we incorporated a trifluoromethyl group in our design to improve the *in vivo* activity,²² resulting in compounds **11** – **14** with varying reactive warheads (Figure 1). The binding affinities of compounds **7**, **11** – **14** were determined using a [³H]-CCR2-RA displacement assay (Table 1). In this assay, all compounds fully displaced the intracellular radioligand [³H]-CCR2-RA in a concentration-dependent manner, displaying high to moderate binding affinities for hCCR2b ($K_i < 100$ nM). Of note, for compounds **11** – **14**, binding affinities are reported as “apparent (p)K_i” values due to the putative covalent interaction between these compounds with CCR2, which precludes the determination of equilibrium binding parameters. The non-covalent control **7** displaced [³H]-CCR2-RA with a pK_i value of 8.2 (Table 1). Of note, substitution of the chlorine group in **7** by trifluoromethyl in **11** – **14** does not affect the affinity towards CCR2, indicating that both groups are equally tolerated; thus we continued using compound **7** as non-covalent control (data not shown). Compound **13** with a non-selective fluorosulfonyl warhead exhibited the highest drop in affinity compared to **7**, with a 15-fold difference in apparent affinity (89 nM). Compound **13** was followed by **11** with the isothiocyanate warhead, which showed a 5-fold reduced affinity compared to **7** (31 nM). Compounds containing an acryloyl (**12**) or thiocyanate (**14**) warhead displayed the highest apparent affinities towards CCR2. Compound **12** displaced [³H]-CCR2-RA with a pK_i of 7.7, while **14** displaced it with a pK_i of 8.4, the highest affinity in this series of compounds (Table 1). Based on the apparent affinities, we decided to continue with compound **14** for further characterization in radioligand binding and functional assays.

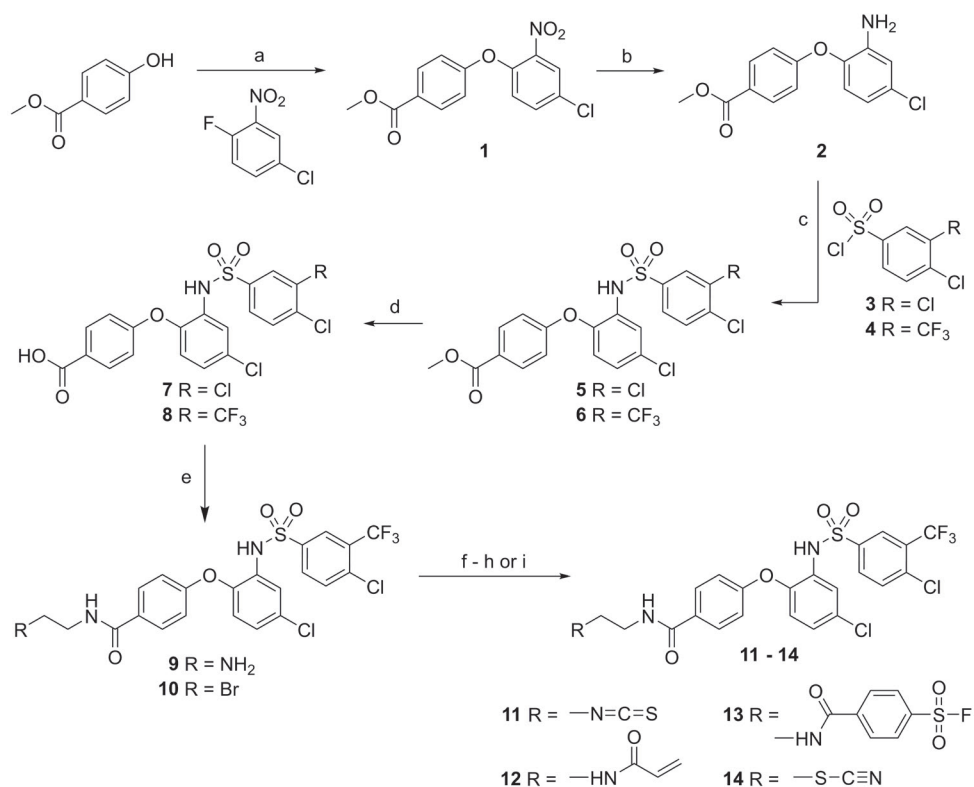


Figure 1. Synthesis of compounds 7, 11 – 14. Final compounds were synthesized using the following reagents and conditions: a) K₂CO₃, DMF, 70°C, 3.5h or overnight; b) SnCl₂·2H₂O, EtOAc, rt, overnight; c) **3**, indium, MeCN, rt, overnight, or **4**, DMAP, pyridine, microwave 95°C, 3h; d) NaOH, dioxane, rt, 2h, or NaOH, dioxane, 60°C, 2.5h; e) i. tert-butyl-N-(2-aminoethyl)carbamate, EDC, HOBt, dioxane, rt; ii. TFA, DCM, rt, for **9**; or 2-bromoethan-1-amine, EDC, HOBt, dioxane, rt for **10**; f) **9**, TEA, CS₂, TsCl, THF for **11**; g) **9**, acryloyl chloride, TEA, acetonitrile, -78°C to rt for **12**; h) **9**, 4-(fluorosulfonyl) benzoic acid, EDC, HOBt, TEA, dioxane, rt for **13**; i) **10**, KSCN, EtOH, reflux, for **14**.

Table 1. Binding affinities (pK_i) of synthesized sulfonamide derivatives determined in [³H]-CCR2-RA displacement assays.

Compound	R ₁	pK _i ± S.E.M (K _i , nM)
7	-	8.2 ± 0.03 (6)
11	Isothiocyanate	7.5 ± 0.04 (31) ^a
12	Acryloylamide	7.7 ± 0.14 (22) ^a
13	(Fluorosulfonyl)phenyl amide	7.2 ± 0.16 (89) ^a
14	Thiocyanate	8.4 ± 0.06 (4) ^a

Data is presented as mean ± S.E.M. of at least three individual experiments performed in duplicate.

^aAs these compounds might bind covalently, we only refer to these affinities as apparent affinities.

Characterization of **14** as covalent probe with radioligand binding assays

Time-dependent characterization of affinity

To determine whether compound **14** binds irreversibly to CCR2, we first determined the time dependency of its affinity, in comparison with the non-covalent control **7**. For this, we measured the affinity of compounds **7** and **14** using a [³H]-CCR2-RA-[R] displacement assay, with a short incubation time of 20 min. In addition, their affinity was measured after a 4 hour pre-incubation of U2OS-CCR2 with increasing concentrations of **7** or **14**, followed by a 20 min co-incubation with [³H]-CCR2-RA-[R] (Figure 2a,b). It is worth to mention that for practical reasons, we switched to using the *R*-isomer [³H]-CCR2-RA-[R] for this and the following assays, instead of the racemic mixture [³H]-CCR2-RA used in the previous section. Compared to the co-incubation experiment, the affinity of non-covalent control **7** remained similar after 4 hour pre-incubation, in agreement with its reversible mode of interaction (Figure 2a and Table 2). In contrast, the affinity of compound **14** increased almost 4 times after pre-incubation, from a K_i of 2.4 nM to 0.7 nM (Table 2), which is apparent as a shift to the left in the concentration-displacement curve (Figure 2b). This indicates that over time, more compound is covalently bound to the receptor, and thus, less of the compound is needed to achieve similar levels of displacement.

Table 2. Time-dependent characterization of affinity (pK_i) of compounds **7 and **14** obtained from [³H]-CCR2-RA-[R] displacement assays.**

Compound	$pK_{i,0h} \pm \text{S.E.M} (K_{i,0h}, \text{nM})^a$	$pK_{i,4h} \pm \text{S.E.M} (K_{i,4h}, \text{nM})^b$	$K_i \text{ shift}^c$
7	$8.4 \pm 0.08 (4.4)$	$8.2 \pm 0.02 (6.1)$	0.7 ± 0.1
14	$8.7 \pm 0.10 (2.4)$	$9.2 \pm 0.15 (0.7)^{**}$	3.8 ± 0.5

Data is presented as mean \pm S.E.M. of at least three individual experiments performed in duplicate. Differences in $pK_{i,0h}$ versus $pK_{i,4h}$ values were analyzed using a paired, two-tailed, Student's *t*-test, with differences as: $**p < 0.01$. ^aAffinity after 20 min co-incubation of unlabeled ligands with [³H]-CCR2-RA-[R] and no pre-incubation. ^bAffinity after 4h pre-incubation with unlabeled ligands followed by 20 min co-incubation with radioligand. ^c K_i -shift: Ratio of $K_{i,4h}/K_{i,0h}$

*Wash-resistant interaction of compound **14** with hCCR2b*

To assess the irreversibility of the interaction with the receptor, we set up a [³H]-CCR2-RA-[R] washout experiment. In this assay we pre-incubated U2OS-CCR2 membranes with $10 \times IC_{50}$ concentration of **7** or **14** for 2 hours, followed by four extensive washing and centrifugation cycles, in order to remove the non-covalently bound ligands. After the washing steps, [³H]-

CCR2-RA-[R] was added and the mix was further incubated for two more hours before measuring radioligand binding. Radioligand binding was compared to the vehicle control, in absence of **7** or **14** (set as 100% binding). [³H]-CCR2-RA-[R] binding was fully recovered in membranes pretreated with **7** (116 ± 8% binding), indicating that this compound was completely washed away during the washing and centrifugation cycles (Figure 2c). In contrast, less than 30% binding of [³H]-CCR2-RA-[R] was measured in membranes pretreated with compound **14** (27 ± 0.4%), indicating that even after extensive washing this compound was still significantly bound to the receptor, prohibiting radioligand binding (Figure 2c). As the thiocyanate warhead of compound **14** reacts selectively with cysteine residues, we performed the same washout assay in the presence of the highly reactive iodoacetamide (IA). IA alkylates the sulfhydryl groups of cysteine residues, making them unavailable for covalent interactions. Thus, before pre-incubation with **7** or **14**, U2OS-CCR2 membranes were pretreated with IA for 30 min in the dark. In presence of IA, binding of [³H]-CCR2-RA-[R] was fully recovered to ~100% for both compounds: 93 ± 5% for compound **14** and 104 ± 5% for compound **7** (Figure 2c). Notably, a comparable effect was observed by pretreating the membranes with 1mM *N*-ethylmaleimide, another common cysteine modifier²³ (data not shown). This loss of wash-resistant capacity of compound **14** in membranes pretreated with IA indicated that cysteine residues were indeed responsible for the irreversible binding of **14** with CCR2.

Characterization of **14** as covalent probe using functional assays

*Characterization of **14** using a [³⁵S]GTPγS binding assay*

After demonstrating that interaction of compound **14** with CCR2 was wash-resistant, we investigated whether this compound was able to inhibit the receptor in a functional assay. First we characterized compounds **7** and **14** in a [³⁵S]GTPγS binding assay. In this assay, both compounds behaved as negative allosteric modulators (NAMs) as they were able to inhibit [³⁵S]GTPγS binding induced by a submaximal concentration of CCL2 (20 nM) in a concentration-dependent manner. The non-covalent control **7** inhibited [³⁵S]GTPγS binding with a pIC₅₀ of 7.0 ± 0.02, while compound **14** showed a higher pIC₅₀ of 7.5 ± 0.04 (Figure 3a and Table 3). Of note, both compounds decreased the basal activity of CCR2 at the highest concentrations (Figure 3a). To evaluate the functional effect of irreversible binding of **14** with CCR2, we set up a [³⁵S]GTPγS washout experiment similar to the previous [³H]-CCR2-RA-[R] washout assay. In this set up, a [³⁵S]GTPγS binding assay was performed after four washing and centrifugation cycles with membranes pretreated with a single concentration

of **7** or **14**. Without the washing steps, both compounds were able to inhibit > 70% of the binding of [³⁵S]GTPγS induced by 20 nM CCL2; in presence of compound **7** [³⁵S]GTPγS binding was reduced to 34 ± 2%, while in presence of compound **14**, [³⁵S]GTPγS binding was fully inhibited to -5 ± 6% (Figure 3b). However, after the four cycles of washing and centrifugation with compound **7**, [³⁵S]GTPγS binding levels recovered to 98 ± 14%, which was comparable to CCL2 alone and significantly different from the “unwashed” situation (*p* < 0.05, Figure 3b), indicating that this compound was effectively washed away in this assay. In contrast, compound **14** remained fully functional after washout, displaying a complete inhibition of [³⁵S]GTPγS binding (-24 ± 30%), which was comparable to the “unwashed” situation (Figure 3b). This confirms that the binding of this compound with CCR2 is wash-resistant, leading to persistent inhibition of the receptor.

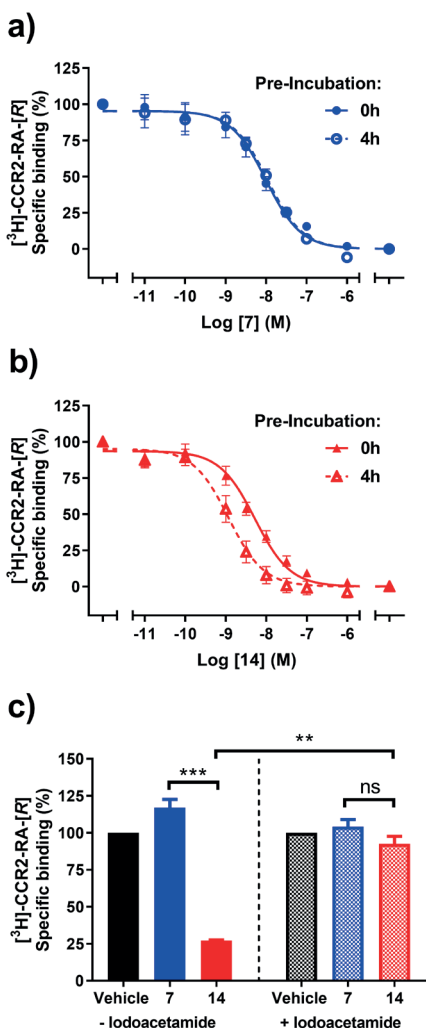


Figure 2. Radioligand binding assays point to a covalent interaction. (a, b) Time-dependent characterization of affinity of **7** (a) and **14** (b). Characterization of affinity in U2OS-CCR2 after i) 20 min co-incubation of unlabeled ligands with [³H]-CCR2-RA-[R] (0h Pre-incubation), and ii) 4h pre-incubation with unlabeled ligands followed by 20 min co-incubation with radioligand. *p*_{K_i} values obtained from these graphs are described in Table 2. (c) Wash-out-radioligand experiments in absence or presence of Iodoacetamide, followed by pre-incubation with 10X IC₅₀ concentration of **7** and **14**. Radioligand binding is recovered when **14** is pre-incubated in U2OS-CCR2 + Iodoacetamide, indicating an interaction with cysteine residues. Data represent the mean ± SEM of at least three independent experiments performed in duplicate.

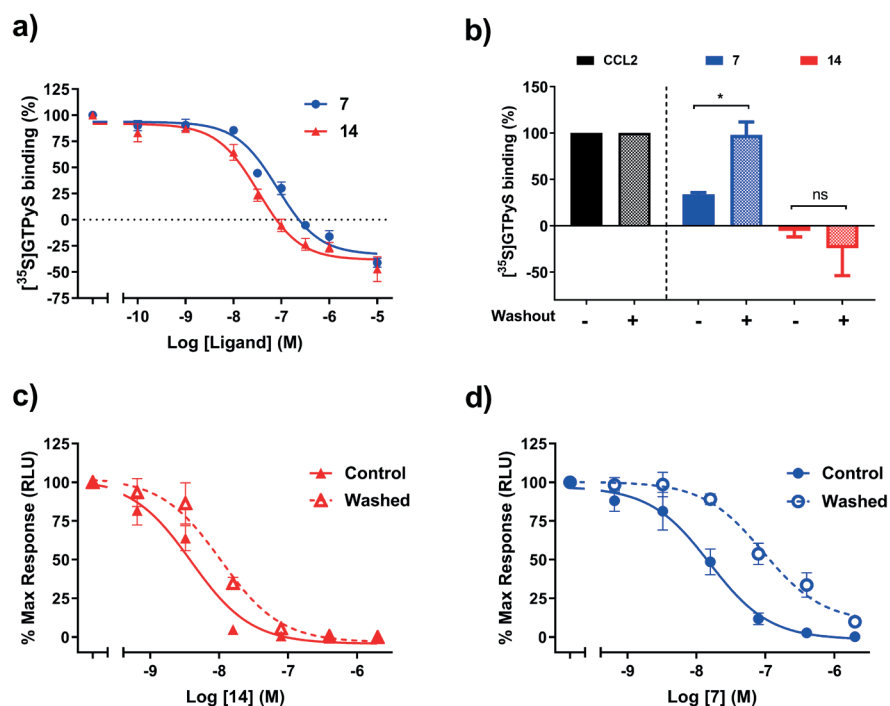


Figure 3. Functional assays point to a covalent interaction. (a) Inhibition of CCL2-stimulated ^{35}S GTPyS binding by increasing concentration of **7** and **14**. (b) After washout, **7** is not able to inhibit ^{35}S GTPyS binding anymore, while **14** remains capable of completely inhibiting ^{35}S GTPyS binding after CCL2 stimulation. (c, d) Inhibition of CCL2-stimulated β -arrestin recruitment by increasing concentrations of **14** (c) and **7** (d) with or without two washing steps before addition of CCL2. Data represent the mean \pm SEM of at least three independent experiments performed in duplicate. pIC_{50} values obtained from these graphs are described in Table 3.

Table 3. Functional characterization of compounds 7 and 14 in hCCR2, obtained in ^{35}S GTPyS and β -arrestin recruitment assays.

Compound	$\text{pIC}_{50} \pm \text{SEM} (\text{IC}_{50}, \text{nM})$		
	^{35}S GTPyS binding ^a	β -arrestin ^b	β -arrestin_washed ^c
7	7.1 ± 0.05 (82)	7.8 ± 0.15 (16)	7.0 ± 0.09 (103)**
14	7.5 ± 0.05 (33)	8.4 ± 0.12 (4)	8.0 ± 0.08 (10)*

Data is presented as mean \pm S.E.M. of at least three individual experiments performed in duplicate. ^aInhibition of ^{35}S GTPyS binding in U2OS-CCR2 at 25 $^{\circ}\text{C}$, after stimulation with 20 nM CCL2. ^bInhibition of β -arrestin recruitment determined with a NanoBit CCR2 assay, after stimulation with 200 nM CCL2. ^cInhibition of β -arrestin recruitment determined with a NanoBit CCR2 assay, after two washing steps followed by stimulation with 200 nM CCL2. Differences in pIC_{50} values between unwashed and washed samples were analyzed using a paired, two-tailed, Student's t-test, with differences as: * $p < 0.05$ and ** $p < 0.01$.

Characterization of 14 using a β -arrestin recruitment assay

Using a NanoBit β -arrestin recruitment assay, we then explored the effect of irreversible binding in a whole-cell functional assay. In this assay, increasing concentrations of **7** or **14** were pre-incubated with HEK293t cells transiently transfected with hCCR2 for 20 min, followed by two washing steps and addition of new medium before incubation with a fixed concentration of CCL2 (200 nM) for another 10 min. In addition, a control experiment was performed using unwashed cells pretreated with **7** or **14**. In the unwashed control situation, **7** and **14** inhibited CCL2-induced β -arrestin recruitment with 5-fold and 8-fold higher potencies, respectively, than those measured in the [35 S]GTP γ S binding assay (Table 3). After two washing steps, compound **7** displayed a pIC_{50} of 7.0 ± 0.09 , corresponding to a 6-fold reduction in potency compared to the unwashed control (pIC_{50} of 7.8 ± 0.15) (Table 3 and Figure 3d). For compound **14**, we observed a smaller shift in potency after the washing steps: from a pIC_{50} of 8.4 ± 0.12 in unwashed cells to a pIC_{50} of 8.0 ± 0.08 after washing, corresponding to a 2.5-fold reduction in potency (Table 3 and Figure 3c).

Cysteine C75 as possible anchor point for covalent interaction

Docking of compound 14 into the crystal structure of hCCR2b

The results from the washout experiment in presence of IA prompted us to investigate the cysteine residue responsible for the irreversible binding of compound **14** with CCR2; thus, we investigated which cysteine residues are in close proximity to the intracellular binding pocket of CCR2. In the crystal structure of hCCR2b-T4L in complex with an orthosteric and an intracellular antagonist (PDB 5T1A, **Chapter 3**¹⁹), there are two cysteine residues in proximity of the crystallized intracellular ligand CCR2-RA-[R], where these compounds also bind: Cys75^{2x37}, within 4Å, and Cys70^{1x60}, at 6.4Å. Additionally, following the removal of T4L and re-building of the native ICL3, we discovered that it contains Cys232^{5x68}, at 14Å from the intracellular binding pocket. Although this distance (14Å) is too large to be spanned by the ethylacetamide linker, we realized that the flexible nature of ICL3 and the resulting protein motions can bring Cys232^{5x68} closer to the pocket. Next, we sought to illustrate that covalent binding of **14** in the allosteric binding pocket is sterically feasible, using molecular docking. A docking model was prepared from the crystal structure of hCCR2b-T4L described in **Chapter 3** and the binding pose of **14** was predicted via covalent docking, assuming that the closest of the three cysteines, Cys75^{2x37}, is the covalent attachment point. The docking study supported a potential covalent interaction of compound **14** with Cys75^{2x37}, as the predicted pose was (i) consistent with the predicted poses of non-covalent analogs from the same series, and (ii) compatible with the linker attachment to Cys75^{2x37}. However, because

Cys70^{1x60} and Cys232^{5x68} are also in proximity to this binding site, and they could be brought even closer via unaccounted-for protein motions, they were included together with Cys75^{2x37} in the subsequent mutagenesis study (Figure 4a).

Site-directed mutagenesis study

To assess which of the three cysteines suggested by docking was responsible for the covalent binding of **14**, single-point mutations to serine were made: C70S^{1x60}, C75S^{2x37} and C232S^{5x68}. These CCR2 mutants, together with a CCR2 wild-type (WT) as control, were transiently transfected into CHO cells. After transfection and membrane preparation, we first determined if these mutations affected the binding of [³H]-CCR2-RA-[R]. For this, we performed [³H]-CCR2-RA-[R] displacement assays, in order to determine the affinity of CCR2-RA-[R] for the mutant and WT receptors (Table 4). Compared to the WT (pIC₅₀ of 7.9 ± 0.06), the affinity of CCR2-RA-[R] was not affected in any of the mutants (Table 4), confirming the integrity of the intracellular pocket in all mutants. In contrast, the affinity of **14** was significantly decreased in both C70S and C75S mutants compared to the WT (pIC₅₀ of 8.8 ± 0.10). In the case of the non-covalent control **7**, opposite effects were observed in C70S and C75S: **7**'s affinity was significantly decreased in C70S and increased in C75S in comparison to the WT (pIC₅₀ of 7.9 ± 0.02). The affinity of both **7** and **14** was not affected in C232S, indicative that this residue is not involved in these compounds' binding (Table 4).

Table 4. Binding affinities (pIC₅₀) of **7 and **14** in the different CCR2 constructs, obtained from [³H]CCR2-RA-[R] displacement assays.**

Construct	pIC ₅₀ ± SEM (IC ₅₀ , nM)		
	7	14	CCR2-RA-[R]
WT	7.9 ± 0.02 (12)	8.8 ± 0.10 (2)	7.9 ± 0.06 (12)
C70S	7.7 ± 0.09 (22)*	8.4 ± 0.04 (4)*	7.9 ± 0.02 (13)
C75S	8.2 ± 0.05 (6)**	8.4 ± 0.10 (5)*	8.0 ± 0.05 (11)
C232S	7.9 ± 0.005 (12)	8.8 ± 0.06 (1)	8.0 ± 0.09 (9)

Data is presented as mean ± S.E.M. of at least three individual experiments performed in duplicate. Differences in pIC₅₀ values compared to WT were analyzed using a One-way ANOVA with Dunnett's posthoc test: *p<0.05 and **p<0.01.

Next, a [³H]-CCR2-RA-[R] washout assay was repeated using membrane preparations from mutant and WT CCR2 (Figure 4b). Similarly as in the washout assays in U2OS-CCR2 membranes, compound **7** was completely washed away from the WT receptor, leading to a full recovery of [³H]-CCR2-RA-[R] binding (~100%), while compound **14** only led to 9%

binding of [³H]-CCR2-RA-[R], in agreement with its irreversible nature (Figure 4b). For compound **7**, full recovery of radioligand binding was observed in the three mutants. In the case of compound **14**, mutants C70S and C232S showed similar [³H]-CCR2-RA-[R] binding levels as the WT receptor, indicating that **14** still binds covalently despite these mutations. However, [³H]-CCR2-RA-[R] binding was significantly increased to 30% in the C75S mutant ($p < 0.0001$), indicating a loss of covalent binding in this mutant. This data indicates that Cys75^{2x37} is responsible for the irreversible nature of compound **14**; yet, the recovery of [³H]-CCR2-RA-[R] binding was not complete, i.e. to similar levels as **7**, indicating that other residues might also be involved in the formation of a covalent bond with **14**, or become involved when Cys75^{2x37} is not available. Of note, serine also contains a nucleophilic hydroxyl group, which might possibly interact with the thiocyanate warhead. Hence, we also mutated Cys75^{2x37} to alanine; however, alanine mutation of this residue (C75A) did not improve the recovery of [³H]-CCR2-RA-[R] binding in comparison with C75S (data not shown), further supporting an interaction with multiple residues.

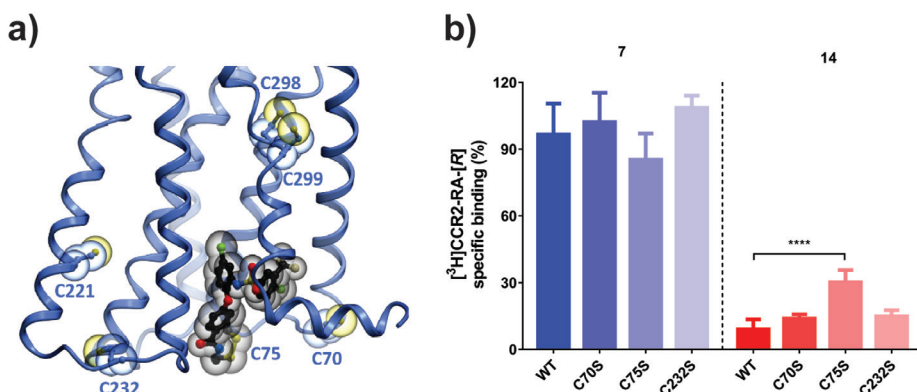


Figure 4. Cysteine 75 seems to be involved in a covalent bond with compound 14. (a) Docking of **14** in the crystal structure of CCR2 (PDB 5T1A, Chapter 3), showing the cysteine residues with potential to interact with this ligand: Cys75^{2x37}, within 4Å; Cys70^{1x60}, at 6.4Å; and Cys232^{5x68}, at 14Å. (b) Washout-radioligand experiments performed after pre-incubation of 60 nM **14** or 200 nM **7** in membranes from CHO cells transiently transfected with CCR2 mutants. Data represent the mean \pm SEM of at least three independent experiments performed in duplicate.

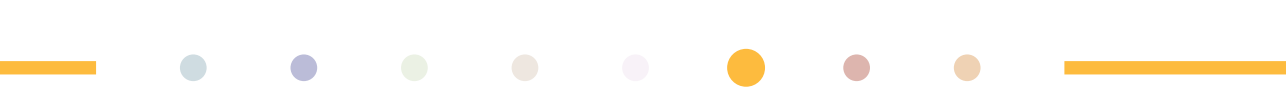
DISCUSSION

Covalent ligands represent useful tool compounds to study the structure and function of GPCRs;^{9, 12} furthermore, due to their 'infinite residence time', covalent inhibitors may lead to enhanced *in vivo* efficacy as a result of their extended duration of action and insurmountability.¹³⁻¹⁵ Several orthosteric and allosteric antagonists have been previously

described for CCR2,²⁴ but no covalent binders have been described so far. Some of these CCR2 antagonists bind to an allosteric binding site located in the intracellular region of the receptor, from where they can inhibit the receptor in a noncompetitive and insurmountable manner.^{19, 25, 26} In an attempt to combine the advantages provided by covalent inhibition and those of intracellular ligands, we aimed to design, synthesize and characterize a novel covalent intracellular ligand for CCR2.

Previous research in our group identified sulfonamide derivatives, similar to compound **7** in our study, as intracellular antagonists for CCR2^{21, 26} (Figure 1). However, Wang *et al.* showed that these sulfonamide derivatives displayed a considerable loss of activity in whole blood assays due to high plasma protein binding.²² Thus, with the aim of developing covalent probes that might be used in both *in vitro* and *in vivo* assays, we replaced the 3,4-dichlorophenyl sulfonamide scaffold of **7** with the 4-chloro-3-(trifluoromethyl)phenyl sulfonamide scaffold (Figure 1), which had shown improved activity in whole blood functional assays.²² Building on this scaffold, we finally introduced several electrophilic warheads connected by a previously described ethylacetamide linker²² (Figure 1). The choice of the electrophilic warhead is based on the desired reactivity towards a target amino acid, as well as the synthetic feasibility to attach it to the scaffold or 'pharmacophore'.¹² Based on the presence of lysine and cysteine residues in the intracellular region of CCR2, we chose four different electrophilic warheads: isothiocyanate, which targets both cysteine and lysine residues;^{27, 28} acryloyl, a Michael acceptor that preferentially targets cysteine over lysine residues;²⁹ a non-selective fluorosulfonyl warhead, with reactivity towards serine, threonine, lysine, tyrosine, lysine, cysteine and histidine residues;³⁰ and a thiocyanate functionality, which selectively reacts with cysteine residues.^{12, 31} As expected, all putative covalent ligands were able to fully displace [³H]-CCR2-RA, indicating that they bind to the same intracellular binding site with high to moderate affinities (Table 1). High affinity is key when designing covalent ligands, as it leads to lower non-specific binding to other nucleophilic residues or off-targets.¹² As only compound **14** with a thiocyanate warhead displayed comparable affinity to the non-covalent control **7** (Table 1), we decided to continue with this compound for further characterization.

It is important to note that equilibrium parameters (K_i/IC_{50} values) are poor indicators of the 'true' binding affinity or potency of covalent ligands, due to their two-step mechanism of inhibition which results in a time-dependent shift in affinity.³² Taking advantage of this notion, we observed a significant increase in the affinity of compound **14** after a 4 hour pre-incubation step in radioligand displacement assays, in comparison with only co-incubation (Figure 2A,B and Table 2). Such increase in binding affinity might be related to an increase in receptor occupancy over time, and thus, to an increase in covalent binding. Similar results have been obtained with covalent ligands targeting other GPCRs.³³⁻³⁵ However, a shift in affinity over time can also be obtained with slowly-dissociating ligands, i.e. long



residence-time ligands, as observed with long residence-time antagonists for CCR5 and CB₁ receptors.^{36,37} Thus, we performed ‘wash-out’ assays, which are commonly used to assess the irreversibility of the interaction with the receptor.³⁸ These assays rely on extensive washing to ensure the removal of unbound ligand, and they have been previously used to validate the irreversible nature of covalent ligands for other GPCRs.^{33-35, 39, 40} After four washing steps, [³H]-CCR2-RA-[R] binding was completely recovered in membranes pretreated with the non-covalent control **7**, while less than 30% [³H]-CCR2-RA-[R] binding was measured in membranes pretreated with compound **14**, indicative of an irreversible interaction with CCR2 (Figure 2C). The fact that radioligand binding was not completely abolished with compound **14** might be related to the assay conditions used in this study, such as ligand concentration, number of washing steps, and incubation times.

To further provide evidence for the covalent nature of compound **14**, we performed functional ‘wash-out’ experiments using two different functional assays: a membrane based [³⁵S]GTPγS assay and a whole cell based β-arrestin recruitment assay (NanoBit assay). These assays showed that, both compounds are able to fully inhibit CCL2-induced G protein-activation and β-arrestin recruitment in CCR2 with high to moderate potencies (Figure 3 and Table 3), confirming their functional profile as negative allosteric modulators (NAMs), similarly as the previously characterized sulfonamide derivative SD-24.²⁶ After extensive washing, CCL2-induced [³⁵S]GTPγS binding was fully restored in membranes pretreated with **7**; however, CCL2 failed to induce [³⁵S]GTPγS binding in membranes pretreated with **14**, indicative again of an insurmountable and irreversible interaction with the receptor (Figure 3B). Of note, both compounds displayed an inverse agonistic behaviour in this assay, also observed with other intracellular ligands (Chapter 4).⁴¹ In addition, the potencies of **7** and **14** to inhibit CCL2-induced β-arrestin recruitment were compared in ‘unwashed’ versus ‘washed’ samples. In this assay both compounds displayed a decrease in potency after the washing steps; however a bigger shift was observed for **7** than for **14** (Figures 3C,D and Table 3). In this regard, the shorter preincubation time in the NanoBit assay—20 min versus 2 hour preincubation time in radioligand binding and [³⁵S]GTPγS assays—might not have been sufficient to allow compound **14** to fully bind CCR2 in an irreversible manner, resulting in the slight reduction of potency. Furthermore, the highly reducing nature of the intracellular environment, i.e. still intact in whole cell experiments, might limit the formation of the disulfide bond between the cysteine residue and the warhead.⁴²

Finally, we sought to determine the target amino acid of the thiocyanate warhead. The radioligand washout assays in the presence of IA indicates that cysteine residues are critical for the irreversible interaction between compound **14** and CCR2, as the irreversible nature of **14** was lost in membranes treated with IA (Figure 2C). Docking of compound **14** into an *in silico* model of CCR2 supports a potential interaction between compound **14** and

Cys75^{2x37}, resulting in a disulfide bond formation; however, the two other residues could not be completely ruled out due to their proximity to the binding site: Cys70^{1x60} and Cys232^{5x68} (Figure 4A). Notably, Cys75^{2x37} is unique to CCR2, as most chemokine receptors possess a serine residue in this position. Therefore, the three cysteine residues were mutated to serine (C70S^{1x60}, C75S^{2x37} and C232S^{5x68}) in order to reduce their nucleophilic nature and prevent the formation of a covalent bond. Radioligand washout assays showed that the irreversibility of compound **14** is only affected in the CCR2-C75S mutant (Figure 4B). However, this mutation did not lead to a full recovery of [³H]-CCR2-RA-[R] binding, as observed with compound **7**, suggesting that compound **14** interacts with multiple nucleophilic residues, not unlike other GPCRs.^{33, 43, 44} In light of these results, further mutational studies are necessary to fully delineate the binding mode and amino acid contacts of **14** within CCR2.

To conclude, we report the design, synthesis and pharmacological characterization of compound **14**, the first intracellular covalent NAM for CCR2. A combination of radioligand binding and functional assays was used to provide evidence of an irreversible interaction between compound **14** and CCR2, which leads to a long-lasting functional effect. Moreover, *in silico* structure-based docking and receptor mutagenesis studies suggest that **14** forms a disulfide covalent bond primarily with Cys75^{2x37}, located in the intracellular binding site of CCR2, although other (secondary) interaction sites are possible. Overall, this compound may represent a useful tool to further study CCR2 structure and function in a variety of *in vitro* and *in vivo* studies, which might ultimately enable a better translation of preclinical findings into successful clinical studies.

MATERIALS AND METHODS

Chemistry

General Methods

All solvents and reagents were purchased from commercial sources and were used without further purification. ^1H spectra were recorded on a Bruker AV 400 MHz liquid spectrometer at room temperature (rt) using CDCl_3 , MeOD or DMSO as a solvent. Chemical shifts are reported in ppm relative to internal standard tetramethylsilane (TMS) or solvent resonance. Purity of the compounds was determined by HPLC with a C18 column (50 × 4.6 mm, 3 μm), flow rate 1.3 mL/min, using gradient 10-90% MeCN/ H_2O (0.1% TFA) and measuring UV absorbance at 254 nm. Reactions were monitored by TLC using Merck TLC Silica gel 60 F₂₅₄ aluminum sheets. Compounds were visualized by UV irradiation or by staining with KMnO_4 solution in H_2O . Biotage Initiator microwave synthesizer was used for the reactions performed in a microwave reactor. For the flash chromatography, Davisil silica gel (40-63 μm) was used. The automatic flash chromatography was performed on an Isolera One Automatic Flash Chromatography System by Biotage with pre-packed flash cartridges (ISCO RediSep or Biotage ZIP Sphere). Mass spectra were measured using a Shimadzu Prominence LCMS-2020 system and a Gemini C18 Phenomenex column (50 × 3 mm, 3 μm).

Synthetic procedure for compound 7

Commercially available methyl 4-hydroxybenzoate (1 eq) and 5-chloro-2-fluoronitrobenzene (1 eq) were dissolved in dimethylformamide (DMF, 1 mL/mmol) together with potassium carbonate (2 eq) in a round-bottom flask. The mixture was stirred at 70°C under nitrogen atmosphere for 3.5 hours. After the solvent was evaporated, the residue was dissolved in EtOAc and washed with water. The organic layer was dried over MgSO_4 and concentrated in vacuum to afford methyl 4-(4-chloro-2-nitrophenoxy)benzoate **1** (13.9 g, 45.1 mmol, 90%). ^1H NMR (400 MHz, DMSO) δ 8.29 (d, J = 2.6 Hz, 1H), 8.03 – 7.96 (m, 2H), 7.86 (dd, J = 8.9, 2.6 Hz, 1H), 7.42 (d, J = 8.9 Hz, 1H), 7.20 – 7.13 (m, 2H), 3.84 (s, 3H).

The product was dissolved in EtOAc (0.05 M) before addition of $\text{SnCl}_2 \cdot 2\text{H}_2\text{O}$ (5 eq.). The reaction was stirred overnight at rt under nitrogen atmosphere. Upon completion, the reaction was quenched with 1M NaOH and extracted with EtOAc. The organic layer was then washed with H_2O and dried over MgSO_4 to yield methyl 4-(2-amino-4-chlorophenoxy)benzoate **2** (4.13 g, 14.9 mmol, 75%). ^1H NMR (400 MHz, DMSO) δ 7.98 – 7.88 (m, 2H), 7.01

– 6.93 (m, 2H), 6.89 (d, $J = 8.5$ Hz, 1H), 6.85 (d, $J = 2.5$ Hz, 1H), 6.57 (dd, $J = 8.5, 2.6$ Hz, 1H), 5.36 (s, 2H).

Next, CH_3CN was used to dissolve the intermediate before addition of indium (0.1 eq) and commercially available 3,4-dichloro-benzenesulfonylchloride **3** (1 eq). The mixture was stirred overnight at rt, after purging the system with nitrogen. The solvents were then evaporated, the residue extracted with EtOAc and washed successively with H_2O and brine. The organic layer was dried over MgSO_4 , filtered and evaporated, after which the product was purified by flash column chromatography (CHCl_3 :petroleum ether 3:1) in order to obtain pure methyl 4-(4-chloro-2-((3,4-dichlorophenyl)sulfonamido)phenoxy)benzoate **5** (3.61 g, 7.41 mmol, 50%). ^1H NMR (400 MHz, DMSO) δ 10.60 (s, 1H), 7.79 (d, $J = 8.8$ Hz, 2H), 7.76 (d, $J = 1.9$ Hz, 1H), 7.59 (d, $J = 8.4$ Hz, 1H), 7.54 (dd, $J = 11.1, 2.2$ Hz, 2H), 7.33 (dd, $J = 8.8, 2.5$ Hz, 1H), 7.07 (d, $J = 8.8$ Hz, 1H), 6.64 (d, $J = 8.8$ Hz, 2H), 3.83 (s, 3H).

Finally, a mix of 2M NaOH (10 mL) dioxane (10 mL) was added to the intermediate and the mixture was stirred at rt for 2h. Solvents were evaporated and the residue was extracted with DCM. The organic layer was extracted with H_2O . The aqueous layers were pooled and acidified with 6M HCl. Filtration of the precipitate gave 1.47 g of 4-(4-chloro-2-((3,4-dichlorophenyl)sulfonamido)phenoxy)benzoic acid **7** (37 mg, 8%). ^1H NMR (400 MHz, DMSO) δ 12.81 (s, 1H), 10.60 (s, 1H), 7.81 (s, 1H), 7.81 – 7.75 (m, 2H), 7.63 (d, $J = 8.4$ Hz, 1H), 7.57 (dd, $J = 8.4, 2.0$ Hz, 1H), 7.51 (d, $J = 2.4$ Hz, 1H), 7.33 (dd, $J = 8.4, 2.4$ Hz, 1H), 7.04 (d, $J = 9.6$ Hz, 1H), 6.63 (d, $J = 8.8$ Hz, 2H); MS: ESI [$\text{M} - \text{H}$]: 469.8; HPLC: 10.2 min.

Synthetic procedure of compound 11

Previously described **2** (1 eq) and commercially available 4-chloro-3-(trifluoro-methyl) benzenesulfonyl chloride **4** (1.1 eq.) were dissolved in pyridine (0.4 M) and *N,N*-dimethylaminopyridine (0.1eq) was added. The mixture was stirred at 95 °C for 3h under microwave irradiation. The mixture was extracted with DCM and the organic layer was washed with aqueous HCl, water and brine. The organic phase was dried over MgSO_4 and evaporated, after which precipitation with DCM and PE gave methyl 4-(4-chloro-2-((4-chloro-3-(trifluoromethyl)phenyl)sulfonamido)phenoxy)benzoate **6** (1.15 g, 63%). ^1H NMR (400 MHz, CDCl_3) δ 8.03 (d, $J = 2.1$ Hz, 1H), 7.93 (d, $J = 8.8$ Hz, 2H), 7.79 (dd, $J = 8.4, 2.1$ Hz, 1H), 7.73 (d, $J = 2.4$ Hz, 1H), 7.51 (d, $J = 8.4$ Hz, 1H), 7.12 (dd, $J = 8.8, 2.5$ Hz, 1H), 7.00 (s, 1H), 6.77 (d, $J = 8.8$ Hz, 1H), 6.65-6.60 (m, 2H), 3.92 (s, 3H).

A mix of 2M NaOH (6 mL) and dioxane (30 mL) was added to the intermediate and the mixture was stirred for 2.5h at 60°C. Upon completion, the reaction was diluted with H_2O and acidified with aqueous HCl. The product was then extracted with EtOAc (2 × 150 ml),

dried over MgSO_4 and evaporated to yield 4-(4-chloro-2-((4-chloro-3-(trifluoromethyl)phenyl)sulfonamido)phenoxy)benzoic acid **8** (1.64 g, 85%). $^1\text{H NMR}$ (400 MHz, CDCl_3) δ 8.03 (d, $J = 1.8$ Hz, 1H), 7.99 (d, $J = 8.6$ Hz, 2H), 7.80 (dd, $J = 8.3, 2.0$ Hz, 1H), 7.76 (d, $J = 2.5$ Hz, 1H), 7.52 (d, $J = 8.4$ Hz, 1H), 7.13 (dd, $J = 8.8, 2.5$ Hz, 1H), 6.98 (s, 1H), 6.80 (d, $J = 8.7$ Hz, 1H), 6.68 – 6.63 (m, 2H).

A mixture of the carboxylic acid **8** (1 eq), *N*-Boc-ethylenediamine (1 eq.), 1-ethyl-3-(3-dimethylaminopropyl)carbodiimide (EDC, 2 eq), and hydroxybenzotriazole (HOBt, 0.1 eq) was dissolved in dioxane (0.015M) and stirred at rt for at least 20 h until completion. The reaction mixture was diluted with EtOAc and the organic phase was washed with water and brine, dried over MgSO_4 and concentrated. The crude product was purified on a silica gel column chromatography with DCM/MeOH to give tert-butyl(2-(4-(4-chloro-2-((4-chloro-3-(trifluoro-methyl)phenyl)sulfonamido)phenoxy)benzamido)ethyl)carbamate (581 mg, 61%). $^1\text{H NMR}$ (400 MHz, CDCl_3) δ 8.10 (d, $J = 1.5$ Hz, 1H), 7.83 (dd, $J = 8.4, 1.8$ Hz, 1H), 7.75 – 7.68 (m, 3H), 7.54 (d, $J = 8.4$ Hz, 1H), 7.46 (s, 1H), 7.33 (s, 1H), 7.08 (dd, $J = 8.8, 2.5$ Hz, 1H), 6.70 (d, $J = 8.8$ Hz, 1H), 6.64 (d, $J = 8.7$ Hz, 2H), 5.07 (s, 1H), 3.56 - 3.53 (m, 2H), 3.40 (d, $J = 4.6$ Hz, 2H), 1.43 (s, 9H).

The Boc-protected compound was dissolved in DCM (0.1 M), and trifluoroacetic acid (TFA, 4 ml/mmol) was added dropwise. The mixture was stirred at rt for 3 h. After completion, the solvents were evaporated and the residue was dissolved in H_2O and alkalinized with 2M NaOH. The aqueous phase was then extracted with EtOAc and washed successively with water and brine. After drying over MgSO_4 and concentration, the residue was taken up in EtOAc and 1M HCl (1ml/mmol) was added. Evaporation gave *N*-(2-aminoethyl)-4-(4-chloro-2-((4-chloro-3-(trifluoromethyl)phenyl)sulfonamido)phenoxy)benzamide hydrochloride **9** (358 mg, 92%). $^1\text{H NMR}$ (400 MHz, MeOD) δ 8.66 (t, 1H), 8.03 (d, $J = 2.1$ Hz, 1H), 7.84 (dd, $J = 8.3, 2.1$ Hz, 1H), 7.75 (d, $J = 8.8$ Hz, 2H), 7.63 (d, $J = 2.5$ Hz, 1H), 7.59 (d, $J = 8.4$ Hz, 1H), 7.21 (dd, $J = 8.8, 2.6$ Hz, 1H), 6.82 (d, $J = 8.8$ Hz, 1H), 6.63 (d, $J = 8.8$ Hz, 2H), 3.64 (q, $J = 5.9$ Hz, 2H), 3.14 (t, $J = 5.9$ Hz, 2H).

This intermediate (1 eq) was dissolved in THF (0.02M) and triethylamine (6 eq) was added. The mixture was cooled to 0 °C before adding carbon disulphide (4 eq) and the reaction mixture was stirred for approximately 2 h at 0 °C until complete conversion to an intermediate. Tosyl chloride (3.5 eq) was added and the mixture was stirred for an additional 19h. The reaction was quenched with a phosphate buffer and the products were extracted into DCM. The organic phase was washed with brine, dried over MgSO_4 and concentrated. The crude compound was purified with flash column chromatography using DCM/MeOH as eluents to yield final compound 4-(4-Chloro-2-((4-chloro-3-(trifluoromethyl)phenyl)sulfonamido)phenoxy)-*N*-(2-isothiocyanatoethyl)benzamide **11** (6 mg, 6%). $^1\text{H NMR}$ (400 MHz, CDCl_3) δ 8.07 (d, $J = 2.1$ Hz, 1H), 7.83 (dd, $J = 8.4, 2.2$ Hz, 1H), 7.72 (d, $J = 2.5$ Hz, 1H), 7.71 – 7.67 (m,

2H), 7.54 (d, $J = 8.4$ Hz, 1H), 7.32 (s, 1H), 7.11 (dd, $J = 8.8, 2.5$ Hz, 1H), 6.75 (d, $J = 8.8$ Hz, 1H), 6.69 – 6.62 (m, 2H), 6.54 (t, $J = 5.9$ Hz, 1H), 3.83 – 3.76 (m, 2H), 3.76 – 3.69 (m, 2H); MS: ESI [M - H]⁻: 587.9; HPLC: 13.0 min.

Synthetic procedure of compound 12

Previously described **9** (1 eq) was dissolved in acetonitrile (5 mL) and cooled to -78°C in an acetone/dry ice bath. Triethylamine (3.5 eq) and acryloyl chloride (1.1 eq) were added. The reaction mixture was then allowed to warm to room temperature and stirred for 2 hours. The mixture was poured into water, acidified with aqueous HCl and the aqueous layer was extracted with ethyl acetate twice. The organic layers were washed with water, dried over MgSO_4 and concentrated. Purification by preparative TLC with EtOAc/acetone 100:1 as an eluent gave final compound N-(2-acrylamidoethyl)-4-(4-chloro-2-((4-chloro-3-(trifluoromethyl)phenyl)sulfonamido)phenoxy)benzamide **12** (10 mg, 20%). ^1H NMR (400 MHz, CDCl_3) δ 8.09 (d, $J = 2.1$ Hz, 1H), 7.82 (dd, $J = 8.4, 2.2$ Hz, 1H), 7.71 (d, $J = 2.1$ Hz, 1H), 7.70 – 7.68 (m, 2H), 7.53 (d, $J = 8.4$ Hz, 1H), 7.44 (s, 1H), 7.43 (s, 1H), 7.09 (dd, $J = 8.8, 2.5$ Hz, 1H), 6.73 (d, $J = 8.8$ Hz, 1H), 6.64 (d, $J = 8.8$ Hz, 2H), 6.51 (s, 1H), 6.30 (dd, $J = 17.0, 1.3$ Hz, 1H), 6.14 (dd, $J = 17.0, 10.2$ Hz, 1H), 5.69 (dd, $J = 10.2, 1.3$ Hz, 1H), 3.60 (s, 4H); MS: ESI [M - H]⁻: 600.0; HPLC: 11.7 min.

Synthetic procedure of compound 13

A mixture of previously described **9** (1 eq), commercially available 4-fluorosulfonylbenzoic acid (1 eq.), EDC (2 eq), and HOBt (0.1 eq) was dissolved in dioxane (0.015M) and stirred at rt for at least 20 h until completion. The reaction mixture was diluted with EtOAc and the organic phase was washed with water and brine, dried over MgSO_4 and concentrated. The crude product was purified on a silica gel column chromatography with DCM/MeOH to give 4-((2-(4-(4-Chloro-2-((4-chloro-3-(trifluoromethyl)phenyl)sulfonamido)phenoxy)benzamido)ethyl) carbamoyl)benzenesulfonyl fluoride **13** (8 mg, 31%). ^1H NMR (400 MHz, CDCl_3) δ 8.07 (s, 4H), 8.06 (d, $J = 2.1$ Hz, 1H), 7.89 (t, $J = 4.4$ Hz, 1H), 7.82 (dd, $J = 8.4, 2.1$ Hz, 1H), 7.71 (d, $J = 2.5$ Hz, 1H), 7.67 (d, $J = 8.8$ Hz, 2H), 7.52 (d, $J = 8.4$ Hz, 1H), 7.30 (s, 1H), 7.10 (dd, $J = 8.8, 2.5$ Hz, 1H), 6.93 (t, $J = 5.2$ Hz, 1H), 6.74 (d, $J = 8.8$ Hz, 1H), 6.65 (d, $J = 8.8$ Hz, 2H), 3.81 – 3.69 (m, 4H); MS: ESI [M - H]⁻: 732.0; HPLC: 12.8 min.

Synthetic procedure of compound 14

A mixture of the carboxylic acid **8** (1 eq), 2-bromoethylamine (1 eq.), EDC (2 eq), and HOBT (0.1 eq) was dissolved in dioxane (0.015M) and stirred at rt for at least 20 h until completion. The reaction mixture was diluted with EtOAc and the organic phase was washed with water and brine, dried over MgSO₄ and concentrated. The crude product was purified on a silica gel column chromatography with EtOAc/petroleum ether to yield N-(2-bromoethyl)-4-(4-chloro-2-((4-chloro-3-(trifluoromethyl)phenyl)sulfonamido)phenoxy)benzamide **10** (62 mg, 51%). ¹H NMR (400 MHz, CDCl₃) δ 8.06 (s, 1H), 7.85 – 7.77 (m, 3H), 7.73 – 7.69 (m, 1H), 7.51 (d, *J* = 8.4 Hz, 1H), 7.09 (dd, *J* = 8.7, 2.5 Hz, 1H), 6.73 (d, *J* = 8.8 Hz, 1H), 6.60 (d, *J* = 8.8 Hz, 2H), 4.44 (t, *J* = 9.5 Hz, 2H), 4.05 (t, *J* = 9.5 Hz, 2H).

Finally, a mixture of KSCN (6 eq.) and the intermediate (1 eq) was dissolved in EtOH (0.025M) and the mixture was refluxed for 3 days. After completion of the reaction the solvent was evaporated and the residue was dissolved in EtOAc, washed with water and brine, dried over MgSO₄ and concentrated. Preparative TLC with DCM/MeOH 25:1 as an eluent gave final compound 4-(4-Chloro-2-((4-chloro-3-(trifluoromethyl)phenyl)sulfonamido)phenoxy)-N-(2-thiocyanatoethyl)benzamide **14** (4 mg, 21%). ¹H NMR (400 MHz, CDCl₃) δ 8.05 (d, *J* = 2.1 Hz, 1H), 7.82 (dd, *J* = 8.4, 2.1 Hz, 1H), 7.73 (d, *J* = 2.5 Hz, 1H), 7.73 – 7.68 (m, 2H), 7.54 (d, *J* = 8.4 Hz, 1H), 7.19 (s, 1H), 7.11 (dd, *J* = 8.7, 2.5 Hz, 2H), 6.75 (d, *J* = 8.8 Hz, 1H), 6.68 – 6.63 (m, 2H), 6.62 (t, *J* = 5.8 Hz, 1H), 3.88 (q, *J* = 6.0 Hz, 2H), 3.26 (t, *J* = 6.0 Hz, 2H); MS: ESI [M - H]⁻: 587.9; HPLC: 12.5 min.

Biology

Chemicals and Reagents

[³H]-CCR2-RA-[R] (specific activity 59.6 Ci mmol⁻¹) was custom-labelled by Vitrox (Placentia, CA) and [³⁵S]GTPγS (specific activity 1250 Ci mmol⁻¹) was purchased from PerkinElmer (Groningen, The Netherlands). The CCR2 ligands CCR2-RA-[R] and JNJ-27141491 were synthesized as previously described.^{45,46} Human CCL2 was purchased from PeproTech (Rocky Hill, NJ). Bovine serum albumin (BSA, fraction V), guanosine 5'-diphosphate (GDP), and iodoacetamide (IA) were from Sigma Aldrich (St. Louis, MO, USA). Pierce™ Bicinchoninic acid (BCA) protein assay kit and Coelenterazine (CTZ-n) were obtained from Thermo Fisher Scientific (Rockford, IL). Polyethyleneimine (PEI) was purchased from Polysciences Inc. (Warrington, Pennsylvania). Tango CCR2-*bla* osteosarcoma cells stably expressing human CCR2b (U2OS-CCR2) were obtained from Invitrogen (Carlsbad, CA). Chinese hamster ovary (CHO) cells were kindly provided by Hans den Dulk (Leiden University, the Netherlands) and

originally obtained from ATCC. All other chemicals were from standard commercial sources.

Plasmids used in the study

pCDNA3.1+ plasmids contacting the FLAG-tagged wild-type human CCR2 and the human CCR2 mutants C70S^{1x60}, C75S^{2x37} and C232S^{5x68} were cloned in-house. The plasmids CCR2b-SmBit and LgBit- β -arrestin1-EE were generous gifts from Asuka Inoue (Graduate School of Pharmaceutical Sciences, Tohoku University, Sendai, Japan). CCR2b-SmBit was obtained by fusing a small C-terminal fragment (residues 185-VTGYRLFEEIL-195) of engineered *Oplophorus gracilirostris* luciferase known as NanoLuc,⁴⁷ with a flexible 15-AA linker (GGSGGGGSGSSSSGG) preceding it, to the C-terminus of human CCR2b in pCDNA3.1+. LgBit- β -arrestin1-EE was obtained by fusing the remaining larger fragment of NanoLuc (27-VFTLEDFVGD WEQTAAYNLD QVLEQGGVSS LLQNLAVSVT PIQRIVRSGE NALKIDIHVIIPYEGLSADQ MAQIEEVFKV VYPVDDHHFK VILPYGTLVI DGVTPNMLNY FGRPYEGIAVFDGKKITVTG TLWNGNKIID ERLITPDGSM LFRVTINS-184) to the N-terminus of clathrin-binding-deficient variant of human β -arrestin1 incorporated in pCAGGS vector, with a flexible 16AA linker GGSGGGGSGSSSSGGT between the two. The EE variant contains two mutations (R392E, R394E) in the clathrin/AP-2-binding motif of β -arrestin1, which leads to better retention at the cell plasma membrane and hence an increased receptor recruitment signal.⁴⁸ All plasmids were propagated in E coli using ampicillin (100 μ g/mL) as a bacterial selection marker.

Cell culture

U2OS-CCR2 and CHO cells were grown as a monolayer in 10-cm \emptyset or 15-cm \emptyset culture plates at 37 °C and 5% CO₂. U2OS-CCR2 were cultured in McCoy's 5A medium containing 10% fetal calf serum (FCS), 2 mM glutamine, 0.1 mM non-essential amino acids, 25 mM HEPES, 1 mM sodium pyruvate, 200 IU/mL penicillin, 200 μ g/mL streptomycin, 100 μ g/mL G418, 40-50 μ g/mL Hygromycin and 125 μ g/mL Zeocin. Empty CHO cells were cultured in DMEM/F12 medium supplemented with 10% (v/v) newborn calf serum, 200 IU/mL penicillin, 200 μ g/mL streptomycin and 2 mM glutamine. HEK293t cells were cultured in DMEM medium supplemented with 10% FCS. All cells were subcultured twice a week, by trypsinization, at a ratio of 1:3 to 1:8 or 1:30 to 1:50 in the case of CHO cells. Dialyzed fetal calf serum was used before membrane preparation of U2OS-CCR2 cells.

Transfections

Transfections of CHO cells with FLAG-tagged WT or mutant CCR2 were performed using a previously described PEI method.²⁶ Briefly, empty CHO cells were grown to ~50% confluence in 15-cm \emptyset culture plates and transfected with a DNA/PEI mixture in 150 mM NaCl solution containing 10 μ g plasmid mixed with PEI (1 mg/ml) at a mass ratio of 1:6. Before transfection, the DNA/PEI mixture was incubated for 20 min and the culture medium of the cells was refreshed. After 24 hours, sodium butyrate (final concentration of 3 mM) was added to the plates to increase receptor expression.⁴⁹ Finally, cells were incubated for another 24 hours at 37 °C and 5% CO₂. HEK293t cells were transiently transfected with CCR2b-SmBit and LgBit- β -arrestin1-EE plasmids using TransIT[®]-LT1 transfection reagent (Mirus Bio, Madison, WI, USA). Empty cells were grown in 6-cm \emptyset culture plates to 60 – 80% confluence before transfection with DNA/reagent mixture, containing 6 μ g plasmid mixed with TransIT[®]-LT1 reagent at a 1:3 ratio. The DNA/reagent mixture was first incubated for 30 min at room temperature and the culture medium of the cells was refreshed before addition. The transfected cells were incubated for another 24 hours at 37 °C and 5% CO₂ before performing the NanoBit assays.

Membrane preparation

Membranes from U2OS-CCR2 or CHO cells transiently transfected with wild-type (WT) human CCR2 or human CCR2 mutants were prepared as previously described, using several centrifugation and homogenization steps.²⁵ Final membrane pellets were resuspended in ice-cold Tris buffer (50 mM Tris-HCl pH 7.4, 5 mM MgCl₂), homogenized with an Ultra Turrax homogenizer (IKA-Werke GmbH & Co. KG, Staufen, Germany) and stored in aliquots of 100 or 250 μ l at -80 °C. A standard BCA protein determination assay was used to measure the membrane protein concentrations (Pierce™ BCA protein assay kit).⁵⁰

Radioligand binding assays

[³H]-CCR2-RA and [³H]-CCR2-RA-[R] binding assays

For all radioligand binding assays, membranes from U2OS-CCR2 cells or CHO cells transiently transfected with WT or mutant CCR2 were first thawed and homogenized using an Ultra Turrax homogenizer (IKA-Werke GmbH & Co. KG, Staufen, Germany). Membranes were then diluted in assay buffer (50 mM Tris-HCl pH 7.4, 5 mM MgCl₂, 0.1% CHAPS) to a final concentration of 5 - 30 μ g membrane protein in a total volume of 100 μ l. For displacement assays, membranes were coincubated for 2 hours at 25 °C with multiple concentrations of

competing ligand, ranging from 0.01 nM to 10 μ M, and a fixed concentration of radioligand (\sim 6 nM [3 H]-CCR2-RA or [3 H]-CCR2-RA-[R]). At this concentration we ensured that total radioligand binding did not exceed 10% of the total radioactivity added, in order to prevent radioligand depletion. In all cases, nonspecific binding was determined using 10 μ M JNJ-27141491. In the case of preincubation experiments, membranes were preincubated for 4 hours with increasing concentrations of competing ligand, before addition of \sim 6 nM [3 H]-CCR2-RA-[R] and further coincubation of 20 minutes. In all assays, incubations were terminated by rapid vacuum filtration through pre-wetted GF/B filterplates using a PerkinElmer FilterMate harvester (Perkin Elmer, Groningen, the Netherlands). Filters were subsequently washed 10 times with ice-cold washbuffer (50 mM Tris-HCl pH 7.4, 5 mM MgCl₂, 0.01% CHAPS) and dried at 55 °C for at least 30 minutes. Finally, filter-bound radioactivity was measured in a P-E 2450 Microbeta² counter (Perkin Elmer) after addition of 25 μ l Microscint scintillation cocktail (Perkin Elmer).

Wash-out assays with [3 H]-CCR2-RA-[R]

For wash-out assays, membrane homogenates (80 – 100 μ g) were preincubated in 1.5-ml Eppendorf tubes with a single concentration of compounds **7** and **14**, in a final volume of 300 μ l assay buffer (50 mM Tris-HCl pH 7.4, 5 mM MgCl₂, 0.1% CHAPS). In the case of wash-out assays in U2OS-CCR2 membranes, a $10 \times IC_{50}$ concentration was chosen for **7** (90 nM) and **14** (12 nM). In the case of wash-out assays in CHO-CCR2 mutant receptor membranes, a concentration of 200 nM **7** and 60 nM **14** was used to ensure a saturating concentration in all mutants despite changes in affinity. In the case of wash-out assays with IA, U2OS-CCR2 membranes were pretreated with 2 mg/ml IA for 30 minutes at room temperature and protected from light, prior to incubation with ligands. After incubation for 2 hours at 25 °C, while shaking at approximately 800 rpm, the mixture was centrifuged at 13,000 rpm for 5 min at 4 °C and the supernatant containing unbound ligand was removed. The remaining pellet was resuspended in 1 ml assay buffer (50 mM Tris-HCl pH 7.4, 5 mM MgCl₂, 0.1% CHAPS) and incubated for an extra 20 minutes before another cycle of centrifugation and washing. After four cycles, the final membrane pellet was resuspended in 300 μ l assay buffer, transferred to test tubes and incubated with 100 μ l of \sim 6 nM [3 H]-CCR2-RA-[R] for 2 hours at 25 °C while shaking. Incubations were terminated by rapid filtration through a pre-wetted Whatman GF/B filter using a Brandel harvester 24 (Brandel, Gaithersburg, MD, USA). Filters were washed three times with 2 ml ice-cold wash buffer (50 mM Tris-HCl pH 7.4, 5 mM MgCl₂, 0.01% CHAPS) and transferred to polyethylene Pony vials (Perkin Elmer) before measurement of filter-bound radioactivity in a Tri-Carb 2810TR Liquid scintillation analyzer (Perkin Elmer).

[³⁵S]GTPγS binding assays

[³⁵S]GTPγS binding assays were performed as previously described.⁴¹ Briefly, U2OS-CCR2 membrane homogenates (10 μg) were diluted in assay buffer (50 mM Tris-HCl pH 7.4, 5 mM MgCl₂, 100 mM NaCl, 1mM EDTA and 0.05% BSA) supplemented with saponin (0.5 mg/ml) and 10 μM GDP to a total volume of 100 μl. To determine the (p)IC₅₀ values of **7** and **14**, membranes were preincubated for 30 minutes at 25 °C with increasing concentrations of ligand in the presence of an EC₈₀ concentration of CCL2 (20 nM), as previously determined.⁴¹ Basal activity was determined in the absence of any ligand or CCL2; maximal activity in the presence of 20 nM CCL2. After addition of 20 μl [³⁵S]GTPγS (0.3 nM), the mixture was incubated for 90 more minutes at 25 °C before stopping the reaction with ice-cold wash-buffer (50 mM Tris-HCl pH 7.4, 5 mM MgCl₂). Filtration and radioactivity measurement was performed as described under “[³H]-CCR2-RA and [³H]-CCR2-RA-[R] binding assays”.

Wash-out assays with [³⁵S]GTPγS

Wash-out assays with [³⁵S]GTPγS were performed as described under “Wash-out assays with [³H]-CCR2-RA-[R]”. Briefly, U2OS-CCR2 membrane homogenates (40 μg) were pre-incubated in the absence or presence of a single concentration of **7** (600 nM) and **14** (250 nM), in a final volume of 400 μl buffer containing 50 mM Tris-HCl (pH 7.4) and 5 mM MgCl₂. After four cycles of centrifugation and washing, the remaining pellets were transferred to test tubes in a final volume of 320 μl containing [³⁵S]GTPγS assay buffer (50 mM Tris-HCl pH 7.4, 5 mM MgCl₂, 100 mM NaCl, 1 mM EDTA and 0.05% BSA), saponin (0.5 mg/ml), GDP (10 μM) and an EC₈₀ concentration of CCL2 (20 nM). For unwashed samples, only the last centrifugation step was performed in order to resuspend the sample in the same volume of 320 μl. All samples were then preincubated for 30 min at 25 °C before addition of 80 μl [³⁵S]GTPγS (0.3 nM). Reaction was stopped after 90 minutes at 25 °C by rapid filtration as described under “Wash-out assays with [³H]-CCR2-RA-[R]”, but using [³⁵S]GTPγS wash-buffer (50 mM Tris-HCl pH 7.4, 5 mM MgCl₂).

NanoBit CCR2 assays

24 hours post-transfection of HEK293t cells with CCR2b-SmBit and LgBit-β-arrestin1-EE plasmids, the cells were detached with PBS/EDTA (0.2 mM), centrifuged and resuspended in assay buffer (1× HBSS, 5 mM HEPES pH 7.2, 0.05% BSA) to a concentration of 1.3×10⁶ cells/ml. The cells were seeded in a round-bottom 96-wells plate (Greiner Bio-One, NC, USA) at 120,000 cells per well in 90 μL assay buffer. Serial dilutions of test compounds in assay buffer, at 10 × final concentrations, were prepared from 10 mM DMSO stocks. Then, 10 μL of assay buffer (unwashed wells) or diluted test compounds (wash-out wells) were added to the

plate. After incubating the plate at room temperature for at least 20 min, cells were washed twice by spinning the plate at $400 \times g$ for 5 min and discarding the supernatant. Afterwards, cells were resuspended in 80 μL assay buffer and transferred to a Falcon™ 96-well black/clear bottom plate (Corning, NY, USA). 10 μL of assay buffer or 10 μL of test compound were added to wash-out and unwashed wells, respectively. 10 μL of coelenterazine (CTZ-n, Fisher Scientific, Waltham, MA, USA), diluted in assay buffer from a 5mM stock in ethanol, was added to the plate to achieve a final concentration of 10 μM and 100 μL final volume in each well. The plate was then incubated at room temperature for approximately 90 min, protected from light. Basal luminescence was read for each well using a PerkinElmer Victor X Light 2030 apparatus (1 sec, no filter). Next, 10 μL of 2 μM CCL2 in assay buffer was added to each well and the cells were further incubated at room temperature for 10 min, protected from light, after which the plate was read again for endpoint luminescence generated by structural complementation.

Molecular modeling and ligand docking

Generation of a model of WT CCR2

The crystal structure of engineered human CCR2 in complex with an orthosteric and an allosteric antagonists (PDB 5T1A,¹⁹ **Chapter 3**) was used as a template for the generation of the CCR2:14 complex model. All modeling and docking was performed in ICM v3.8-7a (Molsoft LLC, San Diego, CA⁵¹). The T4 lysozyme (T4L) fusion protein present in the structure was removed, the mutated residues in the intracellular part of TM6 reverted to WT, and the intracellular loop 3 (ICL3) rebuilt. For rebuilding the ICL3, a peptide containing residues 223:243 of CCR2 was built *ab-initio*, the backbones of residues 223:231,236:243 and the side chains of residues 223:226,241:243 tethered to their respective positions in the crystal structure, the receptor represented as a set of three dimensional (3D) grid maps representing van der Waals, electrostatic, hydrogen bonding, and surface energy potentials, and the peptide conformation was optimized using the biased probability Monte Carlo (BPMC) sampling in internal coordinates as implemented in ICM.⁵¹ The simulation simultaneously optimized the intramolecular energy of the peptide and its interaction with the context potential grid maps. The best scoring conformation of the peptide was merged with the rest of the receptor coordinates, and the system was minimized in its full-atom representation, with harmonic restraints of gradually decreasing strength imposed between the model and either the X-ray coordinates or the best prediction conformations of the *ab initio* modeled ICL3. Towards the end of the optimization, the restraints were released entirely. The simulations were performed in the presence of crystallographic ligands.

Generation of a model of CCR2:14 complex

Alternative conformers of the allosteric pocket in CCR2 were generated by systematic sampling of aliphatic side-chain rotamers and translations of the intracellular ends of TM helices 6 and 7. The conformer that best predicted the binding poses of the sulfonamide series of allosteric CCR2 antagonists (analogous to **14**) was chosen. The binding pose of **14** was predicted by covalent docking in ICM under the assumption that the covalent attachment residue is C75 due to its proximity. For docking, the receptor atoms in the 4Å vicinity of the allosteric pocket were represented as 3D grid potential maps as above, with the exception of C75 for which the explicit representation was used. The covalent bond between **14** and C75 was imposed and the system was sampled as described above to generate a ranked list of alternative conformations for the ligand. Top 10 conformations were merged with the full-atom model of the receptor and re-scored using the ICM ligand scoring function previously optimized for ligand geometry prediction on a diverse benchmark of crystallographic protein-ligand complexes.⁵² The top-scoring pose was selected.

Data analysis

Data analyses were performed using Prism 7.00 (GraphPad software, San Diego, CA, USA). (p)IC₅₀ values from radioligand displacement assays, [³⁵S]GTPγS binding assays and NanoBit assays were obtained by non-linear regression curve fitting into a sigmoidal concentration-response curve using the equation: $Y = \text{Bottom} + (\text{Top} - \text{Bottom}) / (1 + 10^{-(X - \text{LogIC}_{50})})$. pK_i values were obtained from pIC₅₀ values using the ChengPrusoff equation.⁵³ Data are shown as mean ± SEM of at least three individual experiments performed in duplicate. Statistical analyses were performed as indicated. If p-values were below 0.05, observed differences were considered statistically significant.

REFERENCES

1. Bachelier, F.; Ben-Baruch, A.; Burkhardt, A. M.; Combadiere, C.; Farber, J. M.; Graham, G. J.; Horuk, R.; Sparre-Ulrich, A. H.; Locati, M.; Luster, A. D.; Mantovani, A.; Matsushima, K.; Murphy, P. M.; Nibbs, R.; Nomiya, H.; Power, C. A.; Proudfoot, A. E.; Rosenkilde, M. M.; Rot, A.; Sozzani, S.; Thelen, M.; Yoshie, O.; Zlotnik, A. International Union of Basic and Clinical Pharmacology. [corrected]. LXXXIX. Update on the extended family of chemokine receptors and introducing a new nomenclature for atypical chemokine receptors. *Pharmacol Rev* **2014**, *66*, 1-79.
2. Viola, A.; Luster, A. D. Chemokines and their receptors: drug targets in immunity and inflammation. *Annu Rev Pharmacol Toxicol* **2008**, *48*, 171-197.
3. O'Connor, T.; Borsig, L.; Heikenwalder, M. CCL2-CCR2 signaling in disease pathogenesis. *Endocr. Metab. Immune Disord. Drug Targets* **2015**, *15*, 105-118.
4. Bot, I.; Ortiz Zacarias, N. V.; de Witte, W. E.; de Vries, H.; van Santbrink, P. J.; van der Velden, D.; Kroner, M. J.; van der Berg, D. J.; Stamos, D.; de Lange, E. C.; Kuiper, J.; Ilzerman, A. P.; Heitman, L. H. A novel CCR2 antagonist inhibits atherogenesis in apoE deficient mice by achieving high receptor occupancy. *Sci Rep* **2017**, *7*, 52.
5. Kang, Y. S.; Lee, M. H.; Song, H. K.; Ko, G. J.; Kwon, O. S.; Lim, T. K.; Kim, S. H.; Han, S. Y.; Han, K. H.; Lee, J. E.; Han, J. Y.; Kim, H. K.; Cha, D. R. CCR2 antagonism improves insulin resistance, lipid metabolism, and diabetic nephropathy in type 2 diabetic mice. *Kidney Int.* **2010**, *78*, 883-894.
6. Piotrowska, A.; Kwiatkowski, K.; Rojewska, E.; Slusarczyk, J.; Makuch, W.; Basta-Kaim, A.; Przewlocka, B.; Mika, J. Direct and indirect pharmacological modulation of CCL2/CCR2 pathway results in attenuation of neuropathic pain - In vivo and in vitro evidence. *J. Neuroimmunol.* **2016**, *297*, 9-19.
7. Qian, B. Z.; Li, J.; Zhang, H.; Kitamura, T.; Zhang, J.; Champion, L. R.; Kaiser, E. A.; Snyder, L. A.; Pollard, J. W. CCL2 recruits inflammatory monocytes to facilitate breast-tumour metastasis. *Nature* **2011**, *475*, 222-225.
8. Horuk, R. Chemokine receptor antagonists: overcoming developmental hurdles. *Nat Rev Drug Discov* **2009**, *8*, 23-33.
9. Weichert, D.; Gmeiner, P. Covalent molecular probes for class A G protein-coupled receptors: advances and applications. *ACS Chem. Biol.* **2015**, *10*, 1376-1386.
10. Ghosh, A. K.; Samanta, I.; Mondal, A.; Liu, W. R. Covalent inhibition in drug discovery. *ChemMedChem* **2019**, *14*, 889-906.
11. Jones, L. H. Cell permeable affinity- and activity-based probes. *Future Med. Chem.* **2015**, *7*, 2131-2141.
12. Jörg, M.; Scammells, P. J. Guidelines for the synthesis of small-molecule irreversible probes targeting G protein-coupled receptors. *ChemMedChem* **2016**, *11*, 1488-1498.
13. Bauer, R. A. Covalent inhibitors in drug discovery: from accidental discoveries to avoided liabilities and designed therapies. *Drug Discov Today* **2015**, *20*, 1061-1073.
14. González-Bello, C. Designing irreversible inhibitors--worth the effort? *ChemMedChem* **2016**, *11*, 22-30.
15. Baillie, T. A. Targeted covalent inhibitors for drug design. *Angew. Chem. Int. Ed. Engl.* **2016**, *55*, 13408-13421.
16. Hua, T.; Vemuri, K.; Nikas, S. P.; Laprairie, R. B.; Wu, Y.; Qu, L.; Pu, M.; Korde, A.; Jiang, S.; Ho, J. H.; Han, G. W.; Ding, K.; Li, X.; Liu, H.; Hanson, M. A.; Zhao, S.; Bohn, L. M.; Makriyannis, A.; Stevens, R. C.; Liu, Z. J. Crystal structures of agonist-bound human cannabinoid receptor CB₁. *Nature* **2017**, *547*, 468-471.
17. Glukhova, A.; Thal, D. M.; Nguyen, A. T.; Vecchio, E. A.; Jörg, M.; Scammells, P. J.; May, L. T.; Sexton, P. M.; Christopoulos, A. Structure of the adenosine A1 receptor reveals the basis for subtype selectivity. *Cell* **2017**, *168*, 867-877.
18. Apel, A. K.; Cheng, R. K. Y.; Tautermann, C. S.; Brauchle, M.; Huang, C. Y.; Pautsch, A.; Hennig, M.; Nar, H.; Schnapp, G. Crystal structure of CC chemokine receptor 2A in complex with an orthosteric antagonist provides insights for the design of selective antagonists. *Structure* **2019**, *27*, 427-438.

19. Zheng, Y.; Qin, L.; Ortiz Zacarías, N. V.; de Vries, H.; Han, G. W.; Gustavsson, M.; Dabros, M.; Zhao, C.; Cherney, R. J.; Carter, P.; Stamos, D.; Abagyan, R.; Cherezov, V.; Stevens, R. C.; Iljerman, A. P.; Heitman, L. H.; Tebben, A.; Kufareva, I.; Handel, T. M. Structure of CC chemokine receptor 2 with orthosteric and allosteric antagonists. *Nature* **2016**, *540*, 458-461.
20. Ortiz Zacarias, N. V.; Lenselink, E. B.; Iljerman, A. P.; Handel, T. M.; Heitman, L. H. Intracellular receptor modulation: novel approach to target GPCRs. *Trends Pharmacol Sci* **2018**, *39*, 547-559.
21. Peace, S.; Philp, J.; Brooks, C.; Piercy, V.; Moores, K.; Smethurst, C.; Watson, S.; Gaines, S.; Zippoli, M.; Mookherjee, C.; Ife, R. Identification of a sulfonamide series of CCR2 antagonists. *Bioorg. Med. Chem. Lett.* **2010**, *20*, 3961-3964.
22. Wang, G. Z.; Haile, P. A.; Daniel, T.; Belot, B.; Viet, A. Q.; Goodman, K. B.; Sha, D.; Dowdell, S. E.; Varga, N.; Hong, X.; Chakravorty, S.; Webb, C.; Cornejo, C.; Olzinski, A.; Bernard, R.; Evans, C.; Emmons, A.; Briand, J.; Chung, C. W.; Quek, R.; Lee, D.; Gough, P. J.; Sehon, C. A. CCR2 receptor antagonists: optimization of biaryl sulfonamides to increase activity in whole blood. *Bioorg. Med. Chem. Lett.* **2011**, *21*, 7291-7294.
23. Garritsen, A.; Iljerman, A. P.; Beukers, M. W.; Soudijn, W. Chemical modification of adenosine A1 receptors: implications for the interaction with R-PIA, DPCPX and amiloride. *Biochem. Pharmacol.* **1990**, *40*, 835-842.
24. Carter, P. H. Progress in the discovery of CC chemokine receptor 2 antagonists, 2009 – 2012. *Expert Opin. Ther. Pat.* **2013**, *23*, 549-568.
25. Zweemer, A. J.; Nederpelt, I.; Vrieling, H.; Hafith, S.; Doornbos, M. L.; de Vries, H.; Abt, J.; Gross, R.; Stamos, D.; Saunders, J.; Smit, M. J.; Iljerman, A. P.; Heitman, L. H. Multiple binding sites for small-molecule antagonists at the CC chemokine receptor 2. *Mol. Pharmacol.* **2013**, *84*, 551-561.
26. Zweemer, A. J.; Bunnik, J.; Veenhuizen, M.; Miraglia, F.; Lenselink, E. B.; Vilums, M.; de Vries, H.; Gibert, A.; Thiele, S.; Rosenkilde, M. M.; Iljerman, A. P.; Heitman, L. H. Discovery and mapping of an intracellular antagonist binding site at the chemokine receptor CCR2. *Mol. Pharmacol.* **2014**, *86*, 358-368.
27. Burke, T. R.; Bajwa, B. S.; Jacobson, A. E.; Rice, K. C.; Streaty, R. A.; Klee, W. A. Probes for narcotic receptor mediated phenomena. 7. Synthesis and pharmacological properties of irreversible ligands specific for μ or δ opiate receptors. *J. Med. Chem.* **1984**, *27*, 1570-1574.
28. Nakamura, T.; Kawai, Y.; Kitamoto, N.; Osawa, T.; Kato, Y. Covalent modification of lysine residues by allyl isothiocyanate in physiological conditions: plausible transformation of isothiocyanate from thiol to amine. *Chem. Res. Toxicol.* **2009**, *22*, 536-542.
29. Doorn, J. A.; Petersen, D. R. Covalent modification of amino acid nucleophiles by the lipid peroxidation products 4-hydroxy-2-nonenal and 4-oxo-2-nonenal. *Chem. Res. Toxicol.* **2002**, *15*, 1445-1450.
30. Narayanan, A.; Jones, L. H. Sulfonyl fluorides as privileged warheads in chemical biology. *Chem. Sci.* **2015**, *6*, 2650-2659.
31. Yan, F.; Bikbulatov, R. V.; Mocanu, V.; Dicheva, N.; Parker, C. E.; Wetsel, W. C.; Mosier, P. D.; Westkaemper, R. B.; Allen, J. A.; Zjawiony, J. K.; Roth, B. L. Structure-based design, synthesis, and biochemical and pharmacological characterization of novel salvinorin A analogues as active state probes of the kappa-opioid receptor. *Biochemistry* **2009**, *48*, 6898-6908.
32. Strelow, J. M. A perspective on the kinetics of covalent and irreversible inhibition. *SLAS Discov* **2017**, *22*, 3-20.
33. Yang, X.; Dong, G.; Michiels, T. J. M.; Lenselink, E. B.; Heitman, L.; Louvel, J.; Iljerman, A. P. A covalent antagonist for the human adenosine A_{2A} receptor. *Purinergic Signal.* **2017**, *13*, 191-201.
34. Yang, X.; van Veldhoven, J. P. D.; Offringa, J.; Kuiper, B. J.; Lenselink, E. B.; Heitman, L. H.; van der Es, D.; Iljerman, A. P. Development of covalent ligands for G protein-coupled receptors: a case for the human adenosine A(3) receptor. *J. Med. Chem.* **2019**, *62*, 3539-3552.
35. Doornbos, M. L. J.; Wang, X.; Vermond, S. C.; Peeters, L.; Perez-Benito, L.; Trabanco, A. A.; Lavreysen, H.; Cid, J. M.; Heitman, L. H.; Tresadern, G.; Iljerman, A. P. Covalent allosteric probe for the metabotropic glutamate receptor 2: design, synthesis, and pharmacological characterization. *J. Med. Chem.* **2019**, *62*, 223-233.

36. Xia, L.; de Vries, H.; Yang, X.; Lenselink, E. B.; Kyrizaki, A.; Barth, F.; Louvel, J.; Dreyer, M. K.; van der Es, D.; IJzerman, A. P.; Heitman, L. H. Kinetics of human cannabinoid 1 (CB1) receptor antagonists: structure-kinetics relationships (SKR) and implications for insurmountable antagonism. *Biochem. Pharmacol.* **2018**, *151*, 166-179.
37. Swinney, D. C.; Beavis, P.; Chuang, K. T.; Zheng, Y.; Lee, I.; Gee, P.; Deval, J.; Rotstein, D. M.; Dioszegi, M.; Ravendran, P. A study of the molecular mechanism of binding kinetics and long residence times of human CCR5 receptor small molecule allosteric ligands. *Br. J. Pharmacol.* **2014**, *171*, 3364-3375.
38. Mah, R.; Thomas, J. R.; Shafer, C. M. Drug discovery considerations in the development of covalent inhibitors. *Bioorg. Med. Chem. Lett.* **2014**, *24*, 33-39.
39. Moss, S. M.; Jayasekara, P. S.; Paoletta, S.; Gao, Z. G.; Jacobson, K. A. Structure-based design of reactive nucleosides for site-specific modification of the A2A adenosine receptor. *ACS Med Chem Lett* **2014**, *5*, 1043-1048.
40. Picone, R. P.; Khanolkar, A. D.; Xu, W.; Ayotte, L. A.; Thakur, G. A.; Hurst, D. P.; Abood, M. E.; Reggio, P. H.; Fournier, D. J.; Makriyannis, A. (-)-7'-Isothiocyanato-11-hydroxy-1',1'-dimethylheptylhexahydrocannabinol (AM841), a high-affinity electrophilic ligand, interacts covalently with a cysteine in helix six and activates the CB1 cannabinoid receptor. *Mol. Pharmacol.* **2005**, *68*, 1623-1635.
41. Ortiz Zacarías, N. V.; van Veldhoven, J. P. D.; Portner, L.; van Spronsen, E.; Ullo, S.; Veenhuizen, M.; van der Velden, W. J. C.; Zweemer, A. J. M.; Kreekel, R. M.; Oenema, K.; Lenselink, E. B.; Heitman, L. H.; IJzerman, A. P. Pyrrolone derivatives as intracellular allosteric modulators for chemokine receptors: selective and dual-targeting inhibitors of CC chemokine receptors 1 and 2. *J. Med. Chem.* **2018**, *61*, 9146-9161.
42. Rietsch, A.; Beckwith, J. The genetics of disulfide bond metabolism. *Annu. Rev. Genet.* **1998**, *32*, 163-184.
43. Mercier, R. W.; Pei, Y.; Pandarinathan, L.; Janero, D. R.; Zhang, J.; Makriyannis, A. hCB2 ligand-interaction landscape: cysteine residues critical to biarylpyrazole antagonist binding motif and receptor modulation. *Chem. Biol.* **2010**, *17*, 1132-1142.
44. Suga, H.; Sawyer, G. W.; Ehlerf, F. J. Mutagenesis of nucleophilic residues near the orthosteric binding pocket of M1 and M2 muscarinic receptors: effect on the binding of nitrogen mustard analogs of acetylcholine and McN-A-343. *Mol. Pharmacol.* **2010**, *78*, 745-755.
45. Doyon, J.; Coesemans, E.; Boeckx, S.; Buntinx, M.; Hermans, B.; Van Wauwe, J. P.; Gilissen, R. A.; De Groot, A. H.; Corens, D.; Van Lommen, G. Discovery of potent, orally bioavailable small-molecule inhibitors of the human CCR2 receptor. *ChemMedChem* **2008**, *3*, 660-669.
46. Zou, D.; Zhai, H.-X.; Eckman, J.; Higgins, P.; Gillard, M.; Knerr, L.; Carre, S.; Pasau, P.; Collart, P.; Grassi, J. Novel, acidic CCR2 receptor antagonists: from hit to lead. *Lett. Drug. Des. Discov.* **2007**, *4*, 185-191.
47. England, C. G.; Ehlerding, E. B.; Cai, W. NanoLuc: a small luciferase is brightening up the field of bioluminescence. *Bioconjug. Chem.* **2016**, *27*, 1175-1187.
48. Kim, Y.-M.; Benovic, J. L. Differential roles of arrestin-2 interaction with clathrin and adaptor protein 2 in G protein-coupled receptor trafficking. *J. Biol. Chem.* **2002**, *277*, 30760-30768.
49. Cuisset, L.; Tichonicky, L.; Jaffray, P.; Delpech, M. The effects of sodium butyrate on transcription are mediated through activation of a protein phosphatase. *J Biol Chem* **1997**, *272*, 24148-24153.
50. Smith, P. K.; Krohn, R. I.; Hermanson, G. T.; Mallia, A. K.; Gartner, F. H.; Provenzano, M. D.; Fujimoto, E. K.; Goeke, N. M.; Olson, B. J.; Klenk, D. C. Measurement of protein using bicinchoninic acid. *Anal. Biochem.* **1985**, *150*, 76-85.
51. Abagyan, R.; Totrov, M. Biased probability Monte Carlo conformational searches and electrostatic calculations for peptides and proteins. *J Mol Biol* **1994**, *235*, 983-1002.
52. Schapira, M.; Totrov, M.; Abagyan, R. Prediction of the binding energy for small molecules, peptides and proteins. *J Mol Recognit* **1999**, *12*, 177-190.
53. Cheng, Y.; Prusoff, W. H. Relationship between the inhibition constant (K₁) and the concentration of inhibitor which causes 50 per cent inhibition (I₅₀) of an enzymatic reaction. *Biochem. Pharmacol.* **1973**, *22*, 3099-3108.

